THE SOCIETY OF NAVAL ARCHITECTS AND MARINE ENGINEERS
601 Pavonia Avenue, Jersey City, NJ 07306
Paper to be presented at the Propellers '88 Symposium,
Virginia Beach, Virginia, September 20-21, 1988

Calculations, Model Tests and Full Scale Measurements on a Fully Feathering Controllable Pitch Propeller

No.9

C. Kruppa, Member, Institut für Schiffs-und Meerestechnik, Berlin, Germany

H. Pipplies and **W. Faller,** Visitors, Escher Wyss GmbH, Ravensburg, Federal Republic of Germany

ABSTRACT

Two British triple screw cross-channel ferries have been equipped with Escher Wyss controllable pitch propellers of the fully feathering type on the centre shaft. Due to the highly skewed blades the fully feathering position is achieved by gradual pitch increase rather than by the hitherto applied pitch reduction. The performance of the system was predicted on the basis of model tests and monitored during prototype trials, mainly with regard to spindle torque characteristics. The results of the model and full scale measurements are reported and analysed. In addition, the propeller blade forces are determined analytically for the fully feathered condition, applying finite aspect ratio wing theory and advanced viscous flow foil section analysis.

NOMENCLATURE

C_F	blade force coefficient
C_M	blade moment coefficient
C_{Mc}	centrifugal spindle torque coefficient
C_{Mhy} / C_{Mz}	hydrodynamic spindle torque coefficient
$\bar{C}_{Mhy}$	modified hydrodynamic spindle torque coefficient
C_P	pressure coefficient
D	diameter of propeller
J	propeller advance coefficient
J_o	advance coefficient for idling or free-running propeller
n	propeller rate of revolutions
n_o	rate of revolutions for idling or free-running propeller
P	servo pressure
ΔP	differential servo pressure
Δt	time sequence
V_a	propeller advance speed
x,y,z	cartesian coordinate system
x/c	non-dimensional chordwise coordinate
α_{eff}	effective angle of attack
α_{geo}	geometric angle of attack
φ	blade pitch angle measured from zero thrust setting
$\Delta\varphi$	pitch angle change measured from design pitch setting or fully feathered condition
ρ	density of seawater
ρ^*	density of water during model test
ρ_{Blade}	density of full scale propeller material
ρ_{Model}	density of model propeller material

INTRODUCTION

In 1987 two British cross-channel ferries (so-called jumbo ferries), built by Schichau Unterweser AG, Bremerhaven, for P&O European Ferries Ltd., Dover, christened "Pride of Dover" and "Pride of Calais", were put into service (Fig. 1). The vessels are 169 m long, with a beam of 27.8 m and a draught of 6.10 m.

Each ferry is powered by three Sulzer 14-ZAV 40 medium speed diesel engines, working via Tacke reduction gears on three Escher Wyss controllable pitch propellers. The main particulars of the propulsion machinery are:

- Wings
  2 CPPs, each 4.2 m diameter
  160.2 rpm
  7720 kW

- Centre
  1 CPP, 4.0 m diameter
  163.9 rpm
  7720 kW

Fig. 1 Cross-channel ferry "Pride of Dover"

The vessels are equipped with a single aft rudder located behind the centre propeller. If the centre propeller is not required for the actual operating schedule, or is out of order for any reason, the water flow to the rudder would be disturbed and the ship could not, or not efficiently enough, react to rudder manoeuvres. For this reason a controllable pitch propeller (CPP) of the fully feathering type was specified by the owners. With the centre propeller feathered the effectiveness of the rudder is maintained (Fig. 2).

Fig. 2 Triple screw CPP plant with centre propeller in feathering position

Sulzer - Escher Wyss (SEWR) had built in the past a number of CPPs with feathering capability, with blades having no or only little skew. These types of blades permitted the feathering of the blades via and beyond the "astern" condition, the trailing edge facing forward when feathered. Now the requirement of feathering the blades under any operating condition of a triple screw vessel and the shape of the highly skewed blades stipulated the sequence to be changed from the former "ahead"-"zero thrust"-"astern"-"feathering" to a "feathering"-"ahead"-"zero thrust"-"astern" configuration.

The trunnion bearing principle, typical for the more heavily loaded Escher Wyss propellers, permits an extension of the pitch range from the usual 50-60 degrees to 110 degrees without basic changes in the design (Fig. 3 and 4). Details of this hub design are described in references (1) and (2).

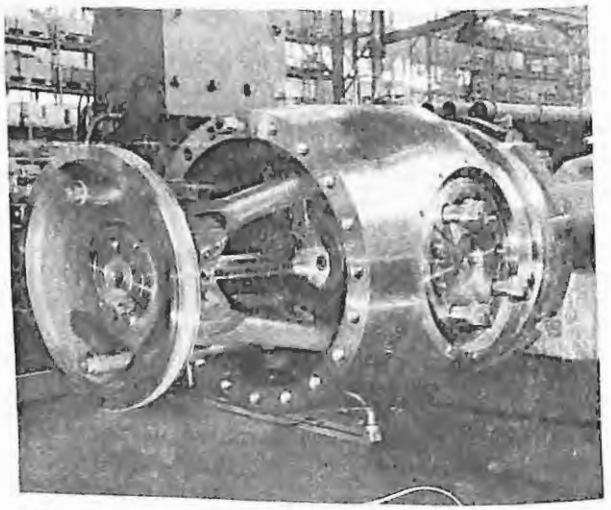

Fig. 3 Propeller hub with feathering capability

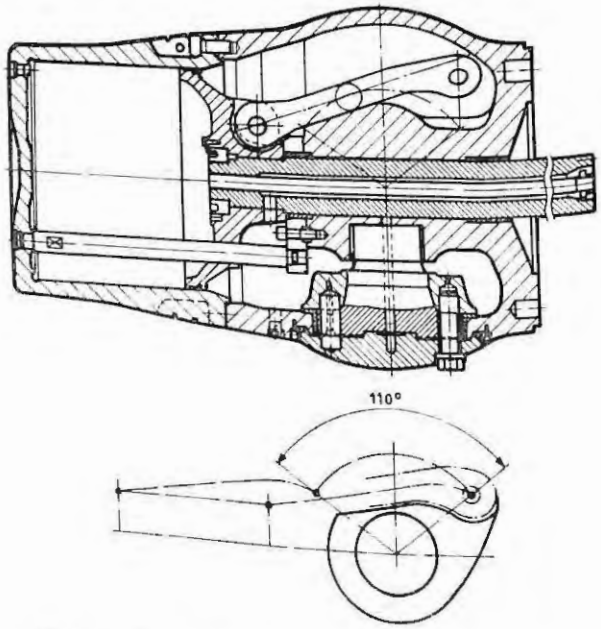

Fig. 4 Trunnion bearing hub with 110 deg. pitch range

In order to know with sufficient accuracy the mechanical loading of the hub components due to the spindle torque in the extreme feathering position, model tests were carried out at the Institut für Schiffs- und Meerestechnik of Technische Universität Berlin. At a later stage the close relationship with owners and builders

opened the possibility to check the test results during prototype sea trials.

The theoretical calculations presented in the following chapter are a by-product of a comprehensive study on advanced profiles and propellers, presently under way at SEWR, concentrating on normal propeller operating conditions, of course, and not on feathered propellers.

THEORETICAL INVESTIGATIONS

The theoretical prediction of extreme off-design pitch blade loads, such as in the feathered position of a CPP, had not been attempted at SEWR so far. When model tests for this condition were to be conducted, it was decided to try a simplified approach based on strip theory.

In a general evaluation of 2-dimensional potential flow and boundary-layer methods some numerical tools were acquired to deal with aero- and hydrodynamic problems. In order to use these for the case at hand, some general assumptions had to be made:

- The inflow to the propeller is supposed to be purely axial and uniform in space and time;
- The flow going through the blade remains in a horizontal plane (no radial induced velocities);
- For a first evaluation, the presence of a hub can be ignored;
- Multhopp's method (3) can be used as a rough approximation for determining the local effective angle of attack, inspite of the low aspect ratio and skew back (sweep) of the blades.

The validity of these assumptions can best be judged by looking at the results in comparison with full scale and model test data. The method adopted cannot replace the model test, yet there would be some potential for refinements, if the need should arise.

In order to use 2-dimensional methods, first the shape of sections that are subjected to the flow has to be determined. Following usual practice, marine propellers are defined by cylindrical sections, pitch, rake and skew distributions. Lacking an analytical method to evaluate arbitrary cuts through the blade, the blade surface was replaced by a number of triangles, the corner points lying on the true surface. The computer then searches for cuts between an arbitrary line in space and every triangle (Fig. 5). As can be seen in Fig. 6, a given set of lines in space (not necessarily in one plane) produces a set of cuts that can be used for a rough section definition.

Cutting through the blade in a systematic way a set of sections is produced (Fig. 7). The distinct S-shape of some sections should be noted. Due to the limited number of triangles (about 2000 in the present case), these sections have to be faired in order to resemble the true blade shape.

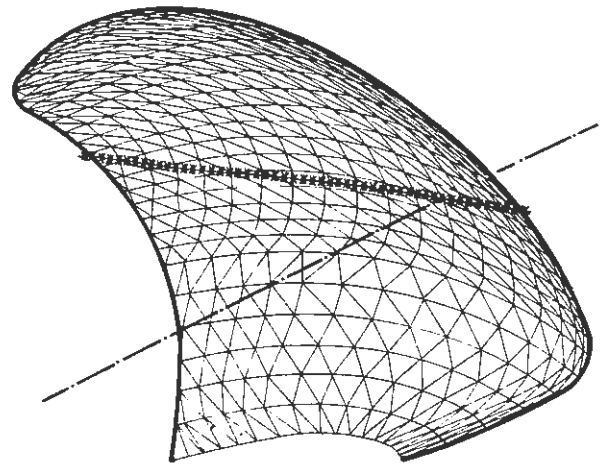

Fig. 5 Blade patch representation

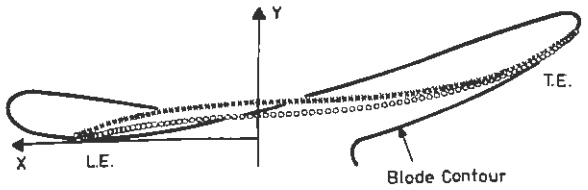

Fig. 6 Planar blade section at z = 1400 mm

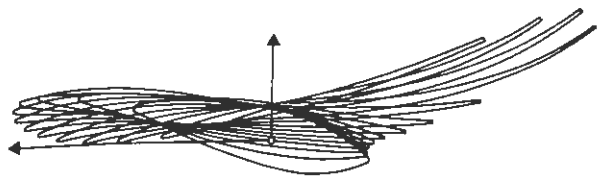

Fig. 7 Set of planar blade sections

Due to 3-dimensional effects, the effective angle of attack of the sections derived will be different from the geometric angle of attack. A

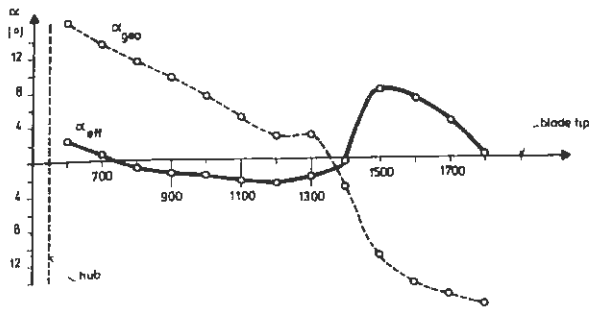

Fig. 8 Blade section inflow geometry

simple method to obtain the relations between bound circulation, induced angle of attack and blade planform is given by Multhopp (3). Fig. 8 shows the results for 13 sections between hub and blade tip.

Using 2-dimensional potential flow theory, pressure distributions for all sections are calculated by the program package of Eppler and Somers (4). The panel method used in this package employs higher order singularities that are quite sensitive to unfaired surfaces. Thus certain spikes in the pressure distribution (Fig. 9) indicate that the fairing of sections mentioned above was not effective enough.

An additional option of the program package allows to perform a displacement thickness iteration using boundary layer theory (5). According to the model test conditions (6), Reynolds numbers for each section have been calculated. Considering their limited values, a considerable extent of laminar flow on the blades of the model propeller can be expected. Therefore the so-called natural transition criterion has been used, which gives relatively extensive laminar flow regions. The adjusted pressure distribution is shown in Fig. 9 together with the profile contour, including the displacement thickness.

Replacing the actual blade by a set of strips with stepwise constant shape (Fig. 10), the calculated pressure distributions, multiplied by their respective areas, are summed up with respect to the general coordinate system (Fig. 11). The resulting forces and moments in non-dimensional form were derived to be as follows:

- Force coefficients

  axial force ('drag')

  $$C_{Fx} = -3.2\ 10^{-3}$$

  lateral force ('lift')

  $$C_{Fy} = 2.7\ 10^{-3}$$

  vertical force

  $$C_{Fz} = 0 \text{ (by definition)}$$

- Moment coefficients

  around x-axis ('shaft torsion')

  $$C_{Mx} = -0.23\ 10^{-3}$$

  around y-axis ('shaft bending')

  $$C_{My} = -1.05\ 10^{-3}$$

  around z-axis ('spindle torque')

  $$C_{Mz} = 2.08\ 10^{-3}$$

As indicated in Fig. 16, the theoretical spindle torque coefficient is about 30 % higher than the coefficient deduced from model tests. The purely potential flow calculation (without Reynolds number effects) gives a slightly higher coefficient ($C_{Mz} = 2.29\ 10^{-3}$).

The program package would allow a large number of additional calculations with varying roughness elements, different transition criteria etc. In order to assess the sensitivity of the procedure to some of the assumptions, a numerical experiment was conducted. First, the presence of the hub was simulated by using the method of images. Secondly, the effect of a slight variation in pitch (+/- 2 degrees) for both configurations was studied. As shown in Fig. 12, using potential flow theory, the pitch for true idling ($C_{Mx} = 0$) is slightly off in both cases: about -1 degree for the simulated hub versus +1 degree for the free blade. Since the spindle torque

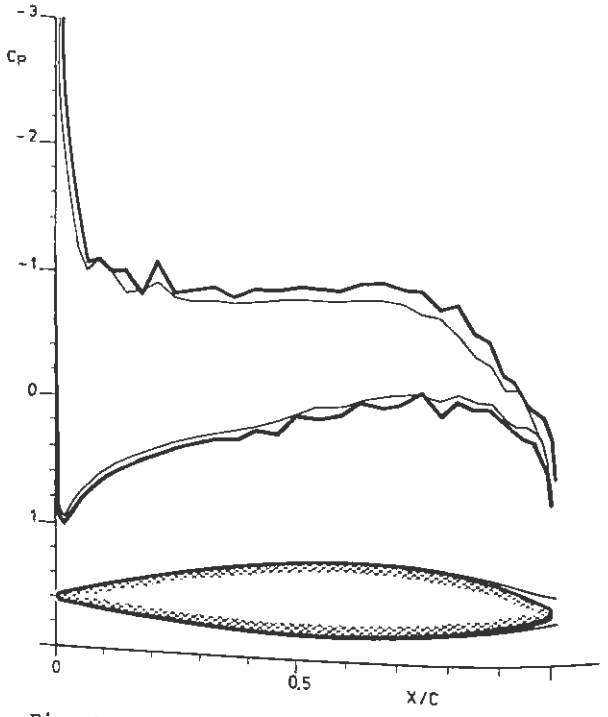

Fig. 9 Pressure distribution at z = 700 mm

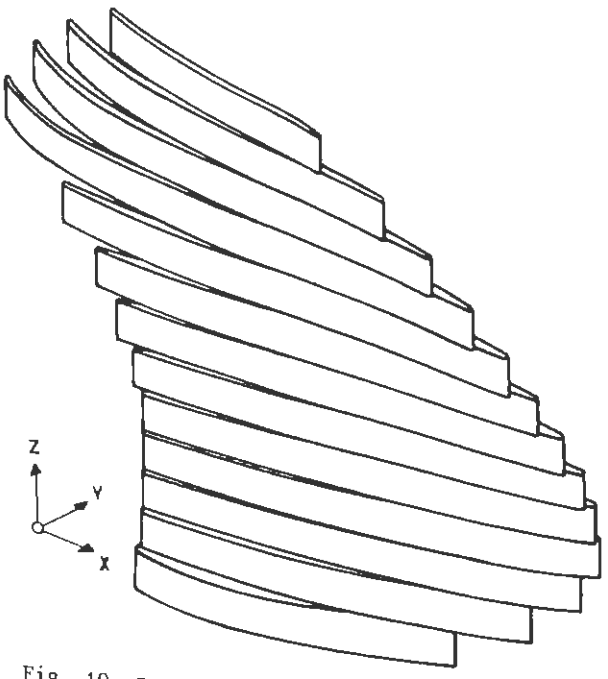

Fig. 10 Strip representation of blade

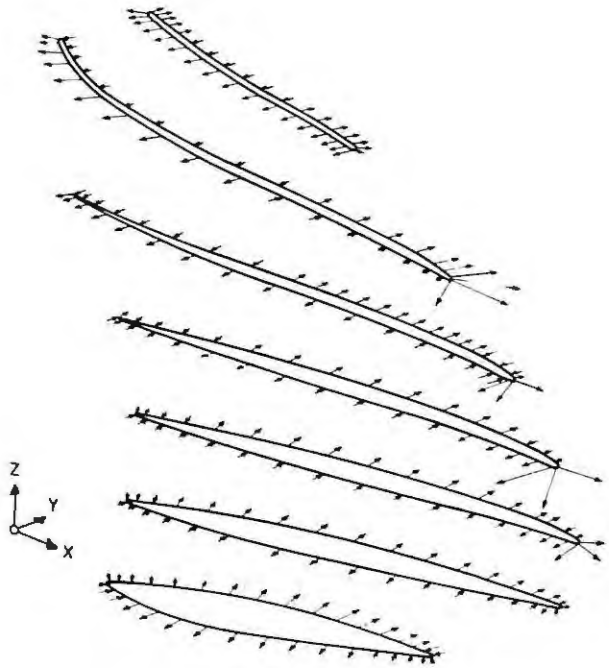

Fig. 11 Blade pressure distribution

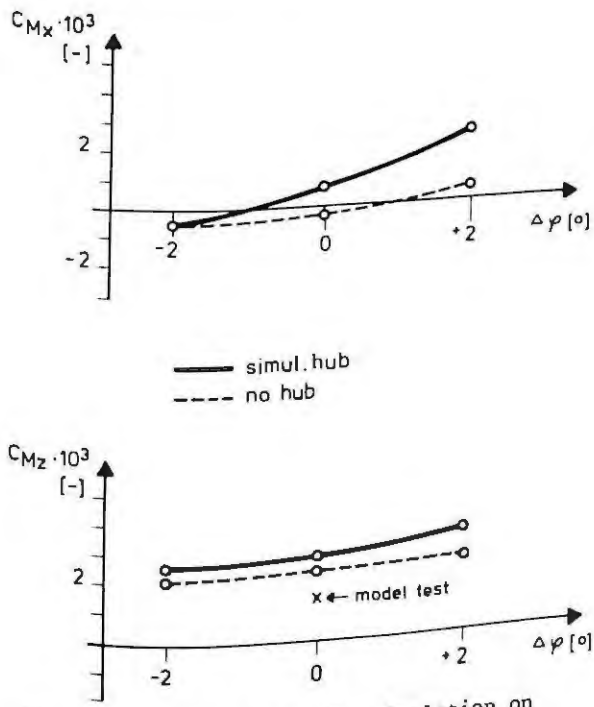

Fig. 12 Influence of hub simulation on moment coefficients

coefficient (C_{Mz}) does not vary too much with pitch, this indicates the inherent limitations of the method.

At the time this study was conducted, no general aircraft-type panel method was available to the authors. Such a method may be a more straightforward way to obtain realistic pressure distributions for the non-rotating blade.

MODEL EXPERIMENTS

Test Set-up

Spindle torque measurements were carried out with a model propeller having a diameter of 250 mm, in the large free surface cavitation tunnel at the Institut für Schiffs- und Meerestechnik of Technische Universität Berlin. The model propeller with detachable blades was supplied by the Vienna Model Basin. For the spindle torque measurements a special hub dynamometer had to be designed and fabricated (Fig. 13), replacing the original solid hub. The hub dynamometer was designed exclusively for spindle torque measurements. Separation of centrifugal and hydrodynamic spindle torque components was achieved by performing separate tests in air. Pitch was changed by means of sets of adaptor flanges attached to the hub.

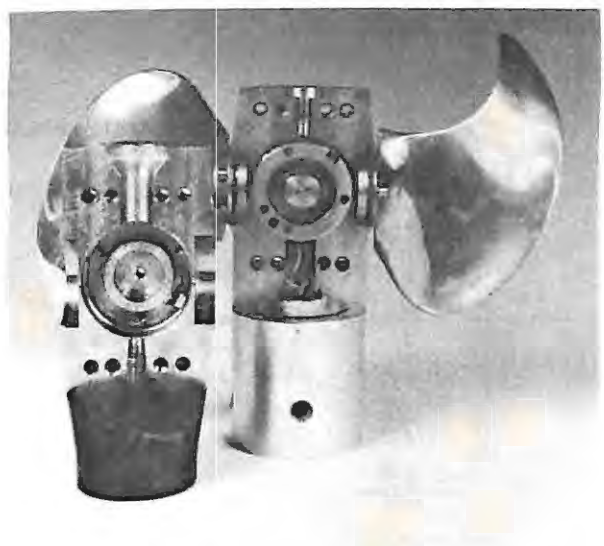

Fig. 13 Spindle torque hub dynamometer

The model propeller was driven by the standard Kempf & Remmers Z-drive dynamometer H 34. Most of the idling (or wind-milling) tests were carried out in open water, with the Z-drive dynamometer serving simply as a propeller shaft support. The dynamometer drive motor was disconnected for this purpose, resulting in only very small frictional torque caused by two bearings.

For the operating propeller a wake field was generated by mesh wire screens. In this case the free water surface in the test section was covered by a rigid plate, generating a closed throat section. The propeller dynamometer was arranged upstream of the mesh wire support frame, driving the propeller from forward through an opening in the screen.

Idling Experiments

For varying pitch settings in terms of $\Delta\varphi$, measured from the design pitch angle at the non-dimensional propeller radius 0.7, the shaft speed n_o was determined for the idling propeller. The results are plotted in Fig. 14 using

the non-dimensional coefficient $1/J_o = n_o D/V_a$. As can be seen, zero rotational speed, and hence the fully feathering condition, is experienced in the vicinity of $\Delta\varphi = 62$ degrees. For negative pitch changes only one measurement was taken at $\Delta\varphi = -20$ degrees, in this case in the simulated wake field.

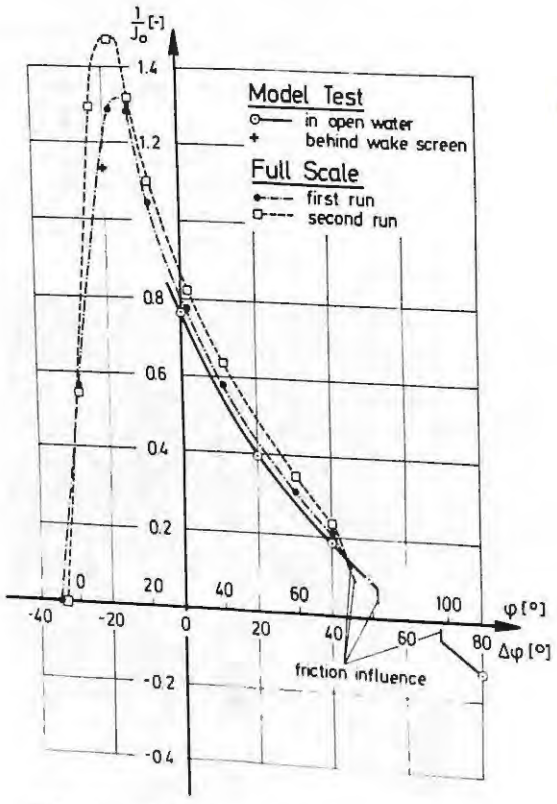

Fig. 14 Idling or free-running characteristic

In order to determine the hydrodynamic spindle torque the centrifugal spindle torque has to be subtracted from the measured value. The latter is negative over the complete operating range of a CPP for positive pitch angles between the zero thrust and the fully feathering condition, thus tending to turn the propeller blade into the zero thrust position. It can be measured by spindle torque tests in air and is dependent on the density of the propeller material, of course. Defining a centrifugal spindle torque coefficient

$$C_{Mc} = \frac{M_{centrifugal}}{\rho^* n^2 D^5},$$

the results of the measurements in air are presented in Fig. 15 (ρ^* = density of tunnel water).

Ideally, the measurements should have yielded a negative centrifugal spindle torque coefficient range of $\pi/2$, e.g. ranging from $\Delta\varphi = -30$ degrees to $\Delta\varphi = 60$ degrees. No explanation can be given for the deficiency apparent in Fig. 15.

The hydrodynamic spindle torque coeffi-

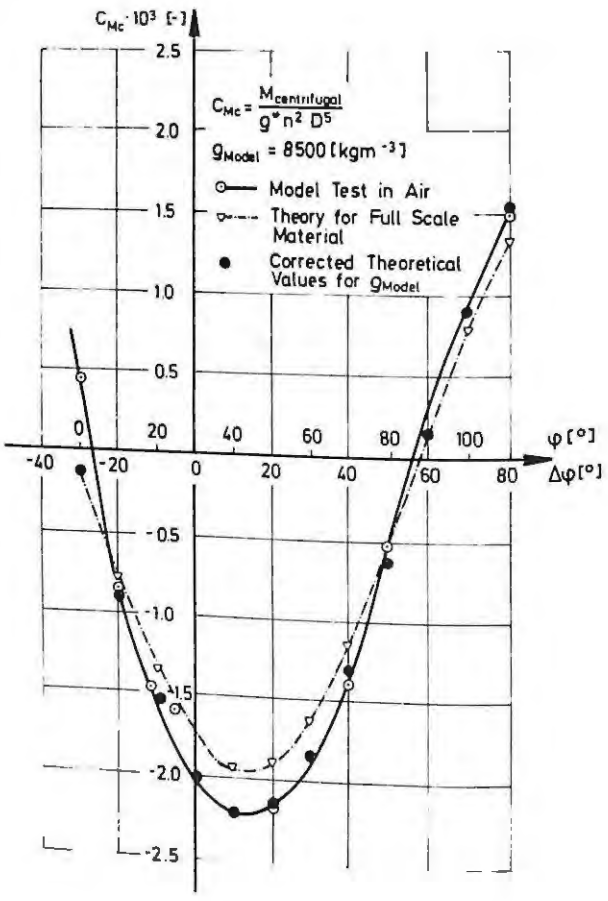

Fig. 15 Centrifugal spindle torque coefficients

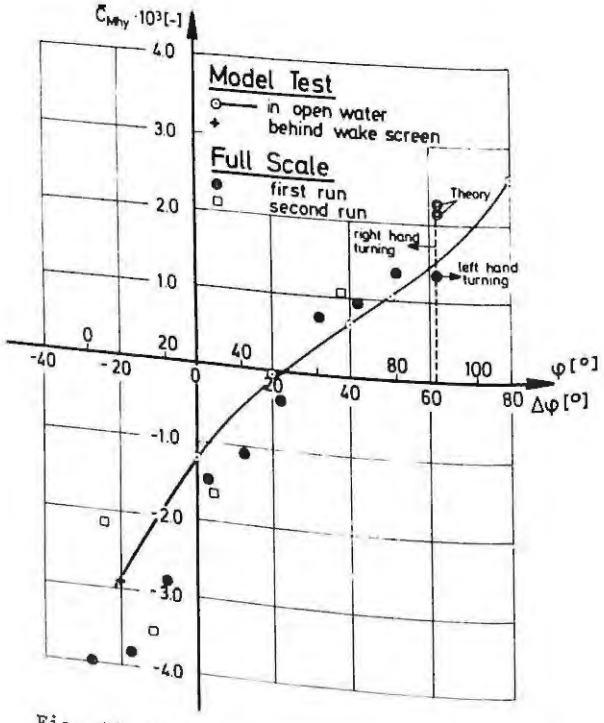

Fig. 16 Modified hydrodynamic spindle torque coefficients

cients, derived with the help of Fig. 15 are

plotted in Fig. 16. However, here the coefficients have been modified, in order to avoid infinite values for the fully feathering position ($n_o \rightarrow o$),

$$\overline{C}_{Mhy} = \frac{C_{Mhy}}{J_o^2} = \frac{M_{hydrodynamic}}{\rho^* V_a^2 D^3} .$$

In order to make use of Fig. 15 and 16 for calculating the total full scale spindle torque the following formula has to be applied:

$$M_{total} = \left[\frac{C_{Mc} \rho_{Blade} \rho^*}{J_o^2 \rho_{Model} \rho} + \overline{C}_{Mhy} \right] \rho V_a^2 D^3$$

where ρ = density of sea water.

Loaded Propeller Tests

Whereas cavitation number was found not to influence the idling experiments it was systematically varied when the propeller was tested under thrusting conditions in the simulated wake field. Hydrodynamic spindle torque coefficients were derived, by subtracting the negative values of the centrifugal component measured in air, and plotted in Fig. 17.

Only at the design pitch setting a larger range of cavitation numbers was investigated. This resulted in marked variations of hydrodynamic spindle torque coefficients, although these occur at higher propeller loading than encountered under actual service conditions.

All the tests carried out at zero test section velocity are suffering from wall interference effects. An exception may be the test under extremely low or zero thrust condition ($\Delta\varphi \sim -30$ degrees).

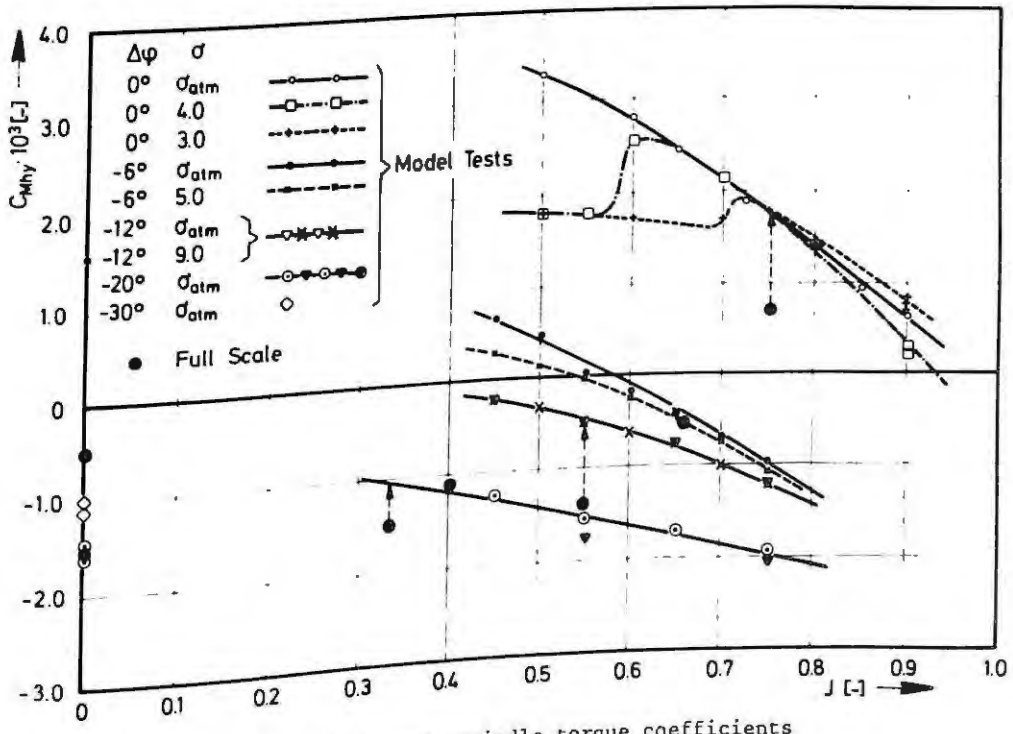

Fig. 17 Hydrodynamic spindle torque coefficients

FULL SCALE MEASUREMENTS

A portable measuring system, existing of a personal computer and an A/D converter, and the necessary instrumentation were brought onboard and connected. The following quantities were measured:

- propeller pitch angle
- shaft speed
- engine power in terms of fuel rack position
- ahead servo pressure
- astern servo pressure.

The main interest was to get knowledge of

- the free-running behaviour of the disengaged centre propeller with the vessel cruising, powered by the wing propulsion systems,
- hard manoeuvring like crash stops,
- setting the pitch to and out of feathering position,
- the pressure requirements of the propeller in holding pitch at various pitch angles.

Free-running Behaviour

The propeller pitch is controlled by an ac-

tuating unit mounted in front of the main reduction gearbox. During the design of this unit the control and the indication of the pitch were omitted for the range between "full ahead" and "feathering", because there is no requirement to control or to know the pitch in this range. For the purpose of a comparison between model results and full scale, the pitch could therefore only be determined on the basis of the time passed after leaving the controlled pitch range and under consideration of the pump capacity.

Shaft speed and pitch angle were plotted for the centre propeller, while the wing shafts were powering the vessel with a speed of about 20 knots. Fig. 18 shows a plot of the actual measurements. A comparison with the model test results can be seen from Fig. 14. The agreement appears to be very good.

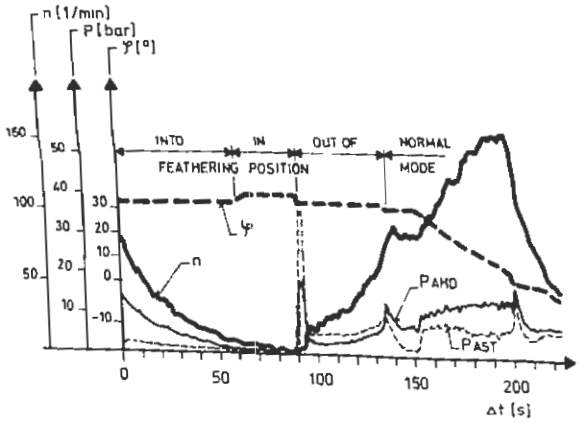

Fig. 18 Feathering manoeuvre [1]

Feathering

Fig. 18 was taken with the pitch setting moving from "ahead" to "feathering" and back. The following quantities are plotted:

- shaft speed
- propeller pitch angle
- ahead servo pressure
- astern servo pressure.

The pressure peak at $\Delta t \sim 90$ s is caused by the motor driven pump which has to be switched on for a short period to initiate the movement of the piston until the PTO-pump delivers sufficient pressure.

Again, time and pump delivery have to be used to determine pitch. The same reasons as mentioned above apply and some calculations have to be made to get a final figure of the servo pressure difference over the pitch angle. Two diagrams, into feathering position and out of feathering position, were plotted one over the other. Mean values can be derived, in this way eliminating the effect of friction to a large extent.

These mean hydraulic pressures are converted to spindle torque coefficients, using a computer program to account for the kinematics in the blade turning mechanism. The total spindle torque coefficient can be split into a centrifugal and a hydrodynamic component. Taking into account that the centrifugal spindle torque coefficient is related to the blade mass distribution only, the values taken either from experiment or from theoretical calculation can be used as a basis. This is confirmed by Fig. 15, where the calculated value is plotted over the curve derived from test results. Since the density of the model propeller and of the full scale propeller are different a correction has to be made. A good agreement is found after correction. Slight differences might be caused by the tolerances of the model propeller.

Subtracting the centrifugal part from the total spindle torque leads to the hydrodynamic part. The result is shown in Fig. 16, where again the model test results are compared with the ones derived from sea trials.

Crash Manoeuvres

Crash stop manoeuvres have been plotted also, an example is given in Fig. 19. By specification, a suppression of windmilling was required which can bee seen very well in the marked up part of the curves. As soon as windmilling is detected the electronic pitch control automatically reduces the speed of pitch change.

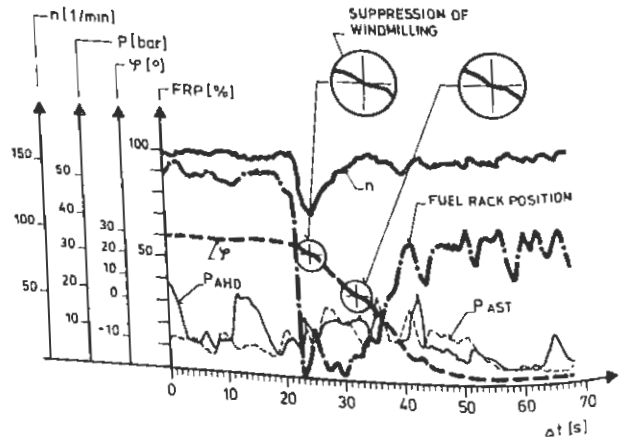

Fig. 19 Crash stop manoeuvre

Pitch Holding Curve

To be able to compare the spindle torque test results of the working propeller with the full scale performance, a so-called pitch holding characteristic was assessed. Starting from astern, the servo pressure and all other necessary quantities were measured with the vessel in

[1] The scale for the pitch angle φ is not valid beyond the design point, for reasons described above. As soon as "feathering" is achieved the record (dotted line) displays a slight discontinuity.

steady state operation, i.e. no more accelerating effects were present. Thus the influence of the friction can be eliminated and a direct relationship between the servo pressure and the spindle torque coefficients can be obtained. Power and shaft speed were measured by members of the Vienna Model Basin.

For five cases also the ship speed was measured. A typical plot of all parameters is shown in Fig. 20. The pitch holding curve, i.e. servo motor differential pressure over the pitch, is shown in Fig. 21. The lower values are regarded to be comparable to the measured model test results, as the higher values occur largely due to additional friction effects. The spindle torque coefficients have been calculated in the same manner as described above. The comparison with the model test results can be seen from Fig. 17.

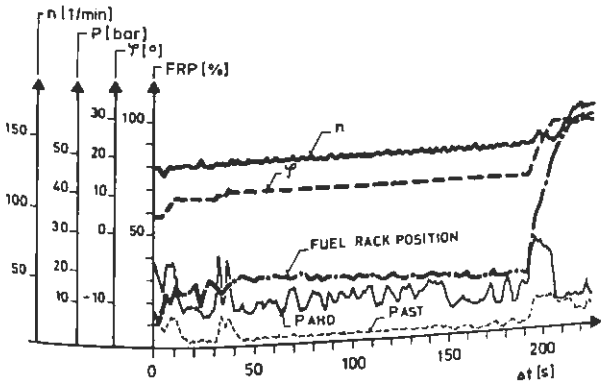

Fig. 20 Standard ahead manoeuvre

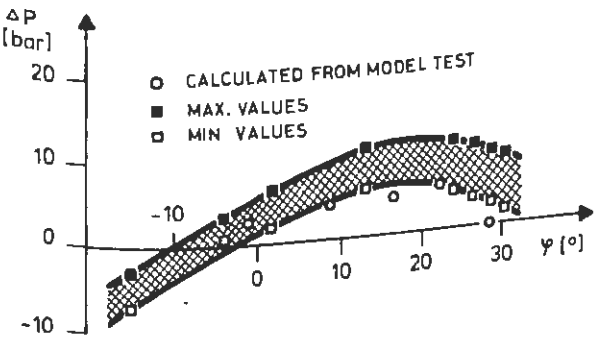

Fig. 21 Pitch holding differential servo pressure

Unfortunately, but not unusual during ship trials, time was not available for more systematic test series. Since the control programs and the time did not allow to vary the propeller advance coefficient only singular points are available for a given pitch. Taking into account all the uncertainties like wake field, wind influence, wave influence, draught, trim of the vessel etc., the agreement in Fig. 17 may be described as acceptable. The comparison may not be regarded as satisfactory by academic standards, but for the practical purposes of a design engineer the model tests represent a reliable tool for assessing spindle torque problems.

ACKNOWLEDGMENTS

The authors would like to thank the owners and builders for the opportunity to perform the full scale measurements, the Vienna Model Basin for assistance during testing and the staff members of the Institut für Schiffs- und Meerestechnik and of Sulzer - Escher Wyss GmbH.

REFERENCES

1. F. Schanz, "Controllable Pitch Propellers", 5th WEGEMT Graduate School on Advanced Ship Power Plant Design and Operation, Berlin, 1981.

2. "Escher Wyss Propellers", Leaflet 21.49.33 RAhe 30.

3. H. Multhopp, "Die Berechnung der Auftriebsverteilung von Tragflügeln", Jahrbuch der Deutschen Luftfahrtforschung, 1938.

4. R. Eppler and D.M. Somers, "A Computer Program for the Design and Analysis of Low-Speed Airfoils", NASA TM 80210, August, 1980.

5. R. Eppler and D.M. Somers, "Supplement to: A Computer Program for the Design and Analysis of Low-Speed Airfoils", NASA TM 81862, December,1980.

6. C. Kruppa, "Verstellmoment-Messungen am Mittelpropeller für DOVER", Institut für Schiffs- und Meerestechnik, Technische Universität Berlin, May, 1987 (unpublished).